

Supplementary Information  
for

# LLDPE-like Polymers Accessible via Ethylene Homopolymerization using Nitro-Appended 2-(Arylimino)Pyridine-Nickel Catalysts

Desalegn Demise Sage<sup>1,2</sup>, Qiuyue Zhang<sup>1</sup>, Ming Liu<sup>1</sup>, Gregory A. Solan<sup>1,3\*</sup>, Yang Sun<sup>1</sup> and Wen-Hua Sun<sup>1,2\*</sup>

<sup>1</sup> Key Laboratory of Engineering Plastics and Beijing National Laboratory for Molecular Sciences, Institute of Chemistry Chinese Academy of Sciences, Beijing 100190, China; desdem0028@iccas.ac.cn (D.D.S.); zhangqiuyue@iccas.ac.cn (Q.Z.); liuming@iccas.ac.cn (M.L.); sy0471103@iccas.ac.cn (Y.S.)

<sup>2</sup> International School, University of Chinese Academy of Sciences, Beijing 100049, China

<sup>3</sup> Department of Chemistry, University of Leicester, University Road, Leicester LE1 7RH, UK

\* Correspondence: gas8@leicester.ac.uk (G.A.S.); Tel.: +44-(0)116-2522096; whsun@iccas.ac.cn (W.-H.S.); Tel.: +86-10-6255-7955

## Table of contents

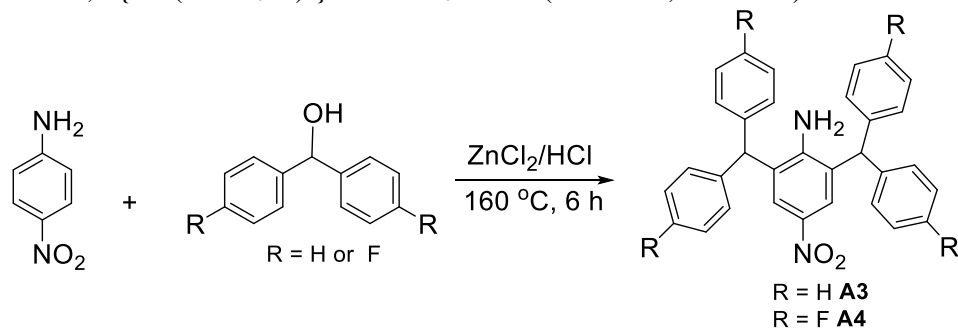
	Page
• <b>Scheme S1</b> Synthetic route to anilines <b>A3</b> and <b>A4</b> .	S2
• <b>Scheme S2</b> Synthetic route to 2,6-diisopropyl-3-nitro-4-(4,4-difluorobenzhydryl)aniline ( <b>A5</b> ).	S3
• <b>Figure S1</b> The three independent molecules (A, B and C) present in the unit cell of <b>Ni3</b> ·xH <sub>2</sub> O (x = 2,3) including three molecules of dichloromethane. Thermal ellipsoids are shown at the 30% probability level, while OH···Br hydrogen bonding interactions between the coordinated water molecules and free bromide ions are shown with dotted lines.	S4
• <b>Figure S2</b> GPC curves of the polyethylene produced using <b>Ni4</b> /MMAO at different molar ratios (runs 1 – 5, Table 4).	S5
• <b>Figure S3</b> GPC curves of the polyethylene produced using <b>Ni4</b> /MMAO at different run temperatures (runs 3, 6 – 8, Table 4).	S5
• <b>Figure S4</b> GPC curves of the polyethylene produced using <b>Ni4</b> /MMAO over different run times (runs 3, 9 – 13, Table 4).	S6
• <b>Figure S5</b> GPC curves of the polyethylene produced using <b>Ni1–Ni5</b> /MMAO under optimum conditions (runs 3, 16 – 19, Table 4).	S6
• <b>Figure S6</b> DSC thermogram of the polyethylene produced using <b>Ni4</b> /MMAO (run 4, Table 4).	S7
• <b>Figure S7</b> <sup>1</sup> H NMR spectrum of the polyethylene sample produced using <b>Ni4</b> /MMAO at 30 °C (run 3, Table 4); recorded at 100 °C in <i>d</i> -C <sub>2</sub> D <sub>2</sub> Cl <sub>4</sub> .	S7
• <b>Figure S8</b> <sup>13</sup> C NMR spectrum of the polyethylene sample produced using <b>Ni4</b> /MMAO at 30 °C including an inset of the δ 110–150 ppm region and a segment of the assigned polymer backbone (run 3, Table 4); recorded at 100 °C in <i>d</i> -C <sub>2</sub> D <sub>2</sub> Cl <sub>4</sub> .	S8
• <b>Figure S9a</b> <sup>1</sup> H NMR spectrum of ligand <b>L1</b> ; recorded in CDCl <sub>3</sub> at ambient temperature.	S9
• <b>Figure S9b</b> <sup>13</sup> C NMR spectrum of ligand <b>L1</b> ; recorded in CDCl <sub>3</sub> at ambient temperature.	S9
• <b>Figure S10a</b> FTIR spectrum of ligand <b>L1</b> .	S10
• <b>Figure S10b</b> FTIR spectrum of complex <b>Ni1</b> .	S10
• <b>Figure S11a</b> <sup>1</sup> H NMR spectrum of ligand <b>L2</b> ; recorded in CDCl <sub>3</sub> at ambient temperature.	S11
• <b>Figure S11b</b> <sup>13</sup> C NMR spectrum of ligand <b>L2</b> ; recorded in CDCl <sub>3</sub> at ambient temperature.	S11
• <b>Figure S12a</b> FTIR spectrum of ligand <b>L2</b> .	S12
• <b>Figure S12b</b> FTIR spectrum of complex <b>Ni2</b> .	S12

• <b>Figure S13</b> $^1\text{H}$ NMR spectrum of aniline <b>A3</b> ; recorded in $\text{CDCl}_3$ at ambient temperature.	S13
• <b>Figure S14a</b> $^1\text{H}$ NMR spectrum of ligand <b>L3</b> ; recorded in $\text{CDCl}_3$ at ambient temperature.	S13
• <b>Figure S14b</b> $^{13}\text{C}$ NMR spectrum of ligand <b>L3</b> ; recorded in $\text{CDCl}_3$ at ambient temperature.	S14
• <b>Figure S15a</b> FTIR spectrum of ligand <b>L3</b> .	S14
• <b>Figure S15b</b> FTIR spectrum of complex <b>Ni3</b> .	S15
• <b>Figure S16</b> $^1\text{H}$ NMR spectrum of aniline <b>A4</b> ; recorded in $\text{CDCl}_3$ at ambient temperature.	S16
• <b>Figure S17a</b> $^1\text{H}$ NMR spectrum of ligand <b>L4</b> ; recorded in $\text{CDCl}_3$ at ambient temperature.	S16
• <b>Figure S17b</b> $^{13}\text{C}$ NMR spectrum of ligand <b>L4</b> ; recorded in $\text{CDCl}_3$ at ambient temperature.	S17
• <b>Figure S18a</b> FTIR spectrum of ligand <b>L4</b>	S17
• <b>Figure S18b</b> FTIR spectrum of complex <b>Ni4</b> .	S18
• <b>Figure S19a</b> $^1\text{H}$ NMR spectrum of aniline <b>A5</b> ; recorded in $\text{CDCl}_3$ at ambient temperature.	S19
• <b>Figure S19b</b> $^{13}\text{C}$ NMR spectrum of aniline <b>A5</b> ; recorded in $\text{CDCl}_3$ at ambient temperature.	S19
• <b>Figure S20a</b> $^1\text{H}$ NMR spectrum of ligand <b>L5</b> ; recorded in $\text{CDCl}_3$ at ambient temperature.	S20
• <b>Figure S20b</b> $^{13}\text{C}$ NMR spectrum of ligand <b>L5</b> ; recorded in $\text{CDCl}_3$ at ambient temperature.	S20
• <b>Figure S21a</b> FTIR spectrum of ligand <b>L5</b> .	S21
• <b>Figure S21b</b> FTIR spectrum of complex <b>Ni5</b> .	S21
• <b>Table S1</b> Crystallographic data for <b>Ni3</b> · $x\text{H}_2\text{O}$ ( $x = 2,3$ ), <b>Ni4</b> and <b>Ni5</b>	S22
• <b>Table S2</b> $^{13}\text{C}$ NMR data of the polyethylene sample produced using <b>Ni4</b> / $\text{EtAlCl}_2$ at 30 °C (run 3, Table 3).	S23
• <b>Table S3</b> Branching analysis for the polyethylene sample produced using <b>Ni4</b> / $\text{EtAlCl}_2$ at 30 °C (run 3, Table 3).	S24
• <b>Table S4</b> $^{13}\text{C}$ NMR data for the polyethylene sample produced using <b>Ni4</b> /MMAO at 30 °C (run 3, Table 4).	S25
• <b>Table S5</b> Branching analysis for the polyethylene sample produced using <b>Ni4</b> /MMAO at 30 °C (run 3, Table 4).	S26
• <b>References</b>	S26

### Preparative details for the anilines (**A3** – **A5**)

As **A1** and **A2** were commercially available (**A1**: CAS number #163704-72-1 and **A2**: CAS number # PH008328), they were used directly for ligand synthesis. The other anilines, 2,6- $\{\text{CH}(\text{C}_6\text{H}_5)_2\}_2$ -4- $\text{NO}_2\text{C}_6\text{H}_2\text{NH}_2$  (**A3**) 2,6- $\{\text{CH}(4\text{-F-C}_6\text{H}_4)_2\}_2$ -4- $\text{NO}_2\text{C}_6\text{H}_2\text{NH}_2$  (**A4**) and 2,6-*i*-Pr<sub>2</sub>-3- $\text{NO}_2$ -4-(4-FPh)<sub>2</sub>C<sub>6</sub>H<sub>2</sub>NH<sub>2</sub> (**A5**), were prepared using routes described below and illustrated in Schemes S1 and S2 below, respectively.

(i) Preparation of 2,6- $\{\text{CH}(4\text{-R-C}_6\text{H}_4)_2\}_2$ -4- $\text{NO}_2\text{C}_6\text{H}_2\text{NH}_2$  (R = H **A3**, R = F **A4**).



**Scheme S1** Synthetic route to anilines **A3** and **A4**.

Based on procedures described in the literature [S1-S4], a mixture of 4-nitroaniline (4.0 g, 29 mmol) and diphenylmethanol (10.7 g, 59.9 mmol) was stirred and heated at 160 °C for 20 min to form a homogeneous melt. Then a solution of  $\text{ZnCl}_2$  (15%) in conc.  $\text{HCl}$  (5 mL) was added dropwise to the melt at a stirring speed of 800 rpm. The reaction mixture was further stirred and heated at 160 °C for a further 7 h. Upon cooling to room temperature, the resulting solid was dissolved in dichloromethane (500 mL).

The solution was washed firstly with aqueous solution of  $\text{NH}_4\text{Cl}$  ( $3 \times 200$  mL) and then secondly with an aqueous solution of  $\text{NaCl}$  ( $2 \times 250$  mL). The organic phase was dried over anhydrous  $\text{MgSO}_4$  and filtered. After evaporation of the majority of the solvent under reduced pressure, the viscous syrup was dissolved in a minimum amount of dichloromethane and recrystallized from excess methanol to afford the desired product **A3** as a yellow crystalline powder (7.6 g, 56%).

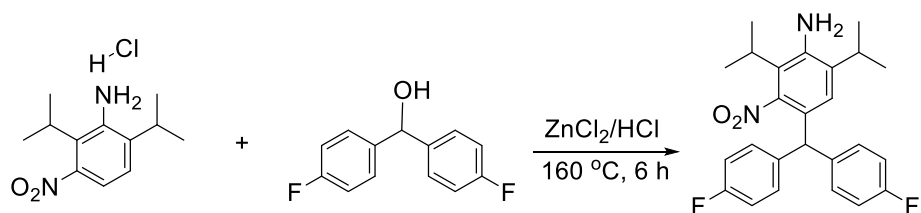
Compound **A3**:  $^1\text{H}$  NMR (400 Hz,  $\text{CDCl}_3$ , TMS):  $\delta$  7.03-6.93 (m, 13H, Ph-H), 6.79-6.78 (m, 8H, Ph-H), 5.05 (s, 2H, -CH-), 3.88 (s, 2H,  $\text{NH}_2$ ).

Similarly, a mixture of 4-nitroaniline (4.0 g, 29 mmol) and bis-(4-fluorophenyl)methanol (12.75 g, 59 mmol) was stirred and heated at  $160^\circ\text{C}$  for 20 min to form a homogeneous melt. Then a solution of  $\text{ZnCl}_2$  (15%) in conc.  $\text{HCl}$  (5 mL) was added dropwise to the melt at a stirring speed of 800 rpm. The reaction mixture was further stirred and heated at  $160^\circ\text{C}$  for a further 7 h. Upon cooling to room temperature, the resulting solid was dissolved in dichloromethane (500 mL). The solution was washed with an aqueous solution of  $\text{NH}_4\text{Cl}$  ( $3 \times 200$  mL) and then an aqueous solution of  $\text{NaCl}$  ( $2 \times 250$  mL). The organic phase was dried over anhydrous  $\text{MgSO}_4$  and filtered. After evaporation of the majority of the solvent under reduced pressure, the viscous syrup was dissolved in a minimum amount of dichloromethane and recrystallized from excess methanol to afford the desired product **A4** as a yellow powder (6.8 g, 43%).

Compound **A4**:  $^1\text{H}$  NMR (400 Hz,  $\text{CDCl}_3$ , TMS):  $\delta$  7.52 (s, 2H), 7.04–7.03 (m, 16H,  $\text{CH}(\text{F-Ph})_2$ ), 5.33 (s, 2H, -CH-), 4.15 (s, 2H,  $\text{NH}_2$ ).

Additionally, the complete characterization data of **A3** and **A4** could be found in references S3 and S4.

(ii) Preparation of 2,6-diisopropyl-3-nitro-4-(4,4-difluorobenzhydryl)aniline (**A5**)



**Scheme S2** Synthetic route to 2,6-diisopropyl-3-nitro-4-(4,4-difluorobenzhydryl)aniline (**A5**)

A mixture of 2,6-diisopropyl-3-nitroaniline hydrochloride (11.7 g, 45.2 mmol) and bis(4-fluorophenyl)methanol (10.15 g, 46.1 mmol) was stirred at  $155^\circ\text{C}$  for 20 min to form a homogeneous melt. Then a solution of  $\text{ZnCl}_2$  (2.35 g, 20%) in conc.  $\text{HCl}$  (5 mL) was added dropwise at a stirring speed of 800 rpm. The reaction mixture was further stirred and heated at  $160^\circ\text{C}$  for further 6 h and then allowed to cool to room temperature. The resulting solid was dissolved in dichloromethane (400 mL) by using an ultra-sonic water bath and washed with aqueous solution of  $\text{NH}_4\text{Cl}$  ( $3 \times 200$  mL) and then an aqueous solution of  $\text{NaCl}$  ( $2 \times 200$  mL). The organic phase was dried with anhydrous  $\text{MgSO}_4$ , filtered and then evaporated under reduced pressure to give a brown viscous residue. This residue was recrystallized by dissolving in a minimum amount of dichloromethane, followed by the addition of excess methanol to afford the desired product as a yellow powder (16.26 g, 85%).

**A5:**  $^1\text{H}$  NMR (400 Hz,  $\text{CDCl}_3$ , TMS):  $\delta$  7.01–6.93 (m, 8H,  $\text{CH}(\text{F-Ph})_2$ ), 6.64 (s, 1H), 5.32 (s, 1H,  $-\text{CH}-$ ), 3.95 (s, 2H,  $\text{NH}_2$ ), 2.98–2.90 (m, 1H,  $-\text{CH}-$ ), 2.86–2.79 (m, 1H,  $-\text{CH}-$ ), 1.38–1.36 (d,  $J = 8.0$ , 6H,  $-\text{CH}_3$ ), 1.12–1.10 (d,  $J = 8.0$ , 6H,  $-\text{CH}_3$ ).

$^{13}\text{C}$  NMR (100 MHz,  $\text{CDCl}_3$ , TMS):  $\delta$  162.8, 160.4, 150.4, 141.3, 138.4, 138.3, 134.4, 130.6, 130.5, 125.2, 122.9, 121.2, 115.3, 115.1, 49.5, 49.5, 28.6, 27.8, 22.0, 19.8.

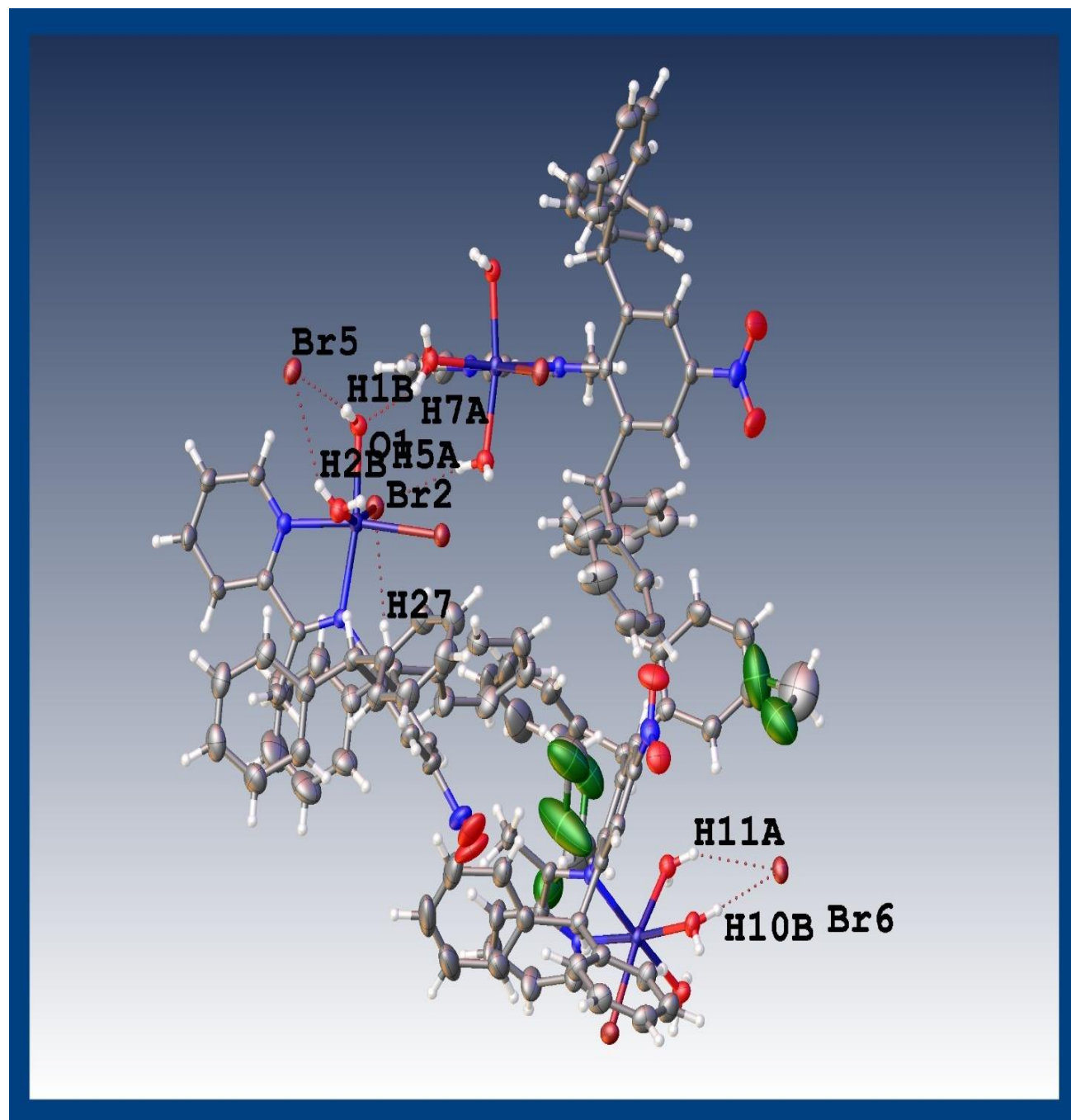


**Figure S1** The three independent molecules (A, B and C) present in the unit cell of  $\text{Ni3} \cdot x\text{H}_2\text{O}$  ( $x = 2,3$ ) including three molecules of dichloromethane. Thermal ellipsoids are shown at the 30% probability level while  $\text{OH} \cdots \text{Br}$  hydrogen bonding interactions between the coordinated water molecules and free bromide ions are shown with dotted lines.

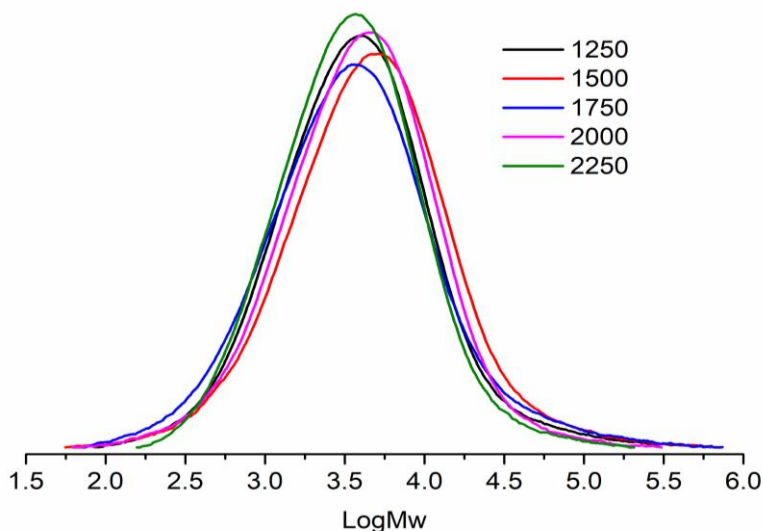


**Figure S2** GPC curves of the polyethylene produced using  $\text{Ni4}/\text{MMAO}$  at different molar ratios (runs 1 – 5, Table 4).

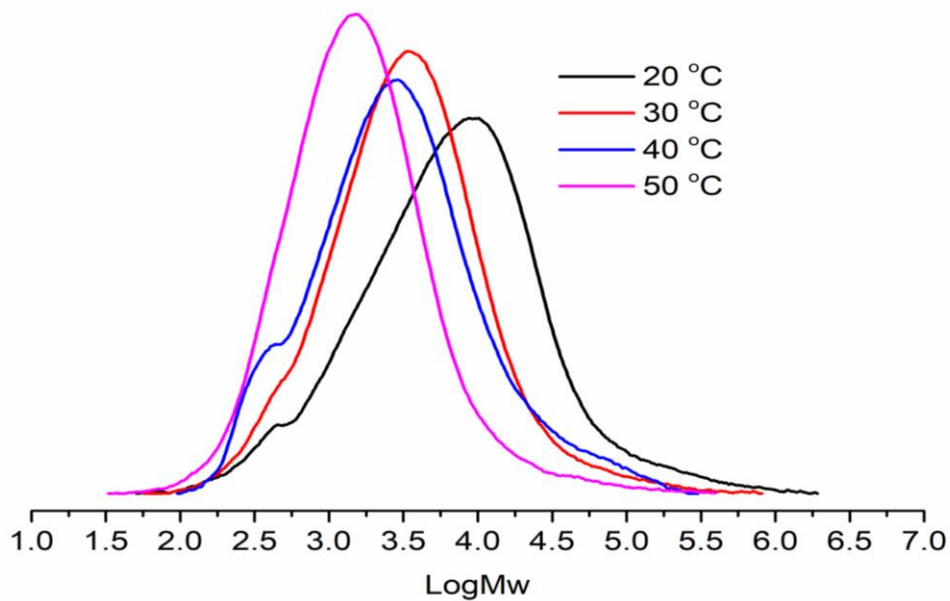


**Figure S3** GPC curves of the polyethylene produced using  $\text{Ni4}/\text{MMAO}$  at different run temperatures (runs 3, 6 – 8, Table 4).

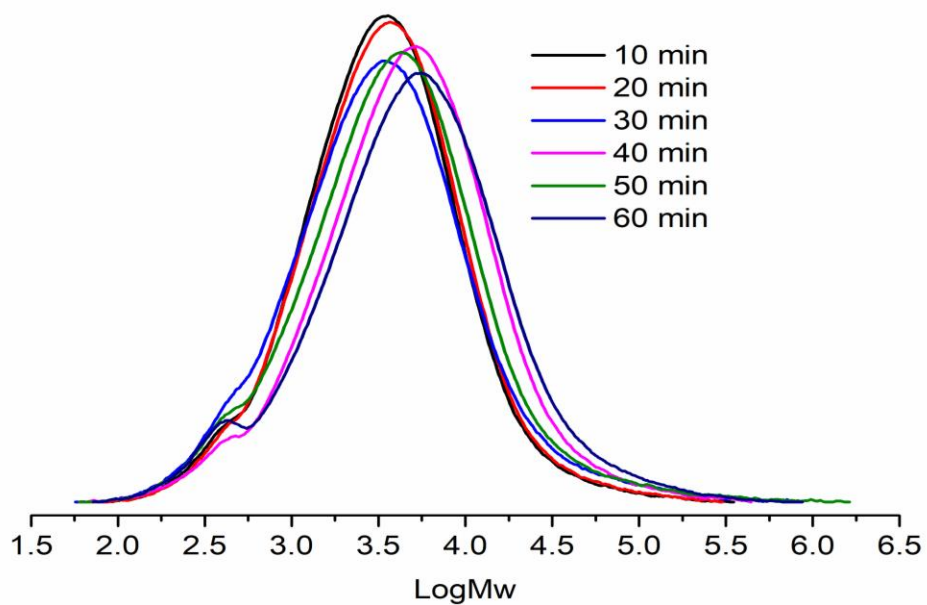


**Figure S4** GPC curves of the polyethylene produced using **Ni4**/MMAO over different run times (runs 3, 9 – 13, Table 4).

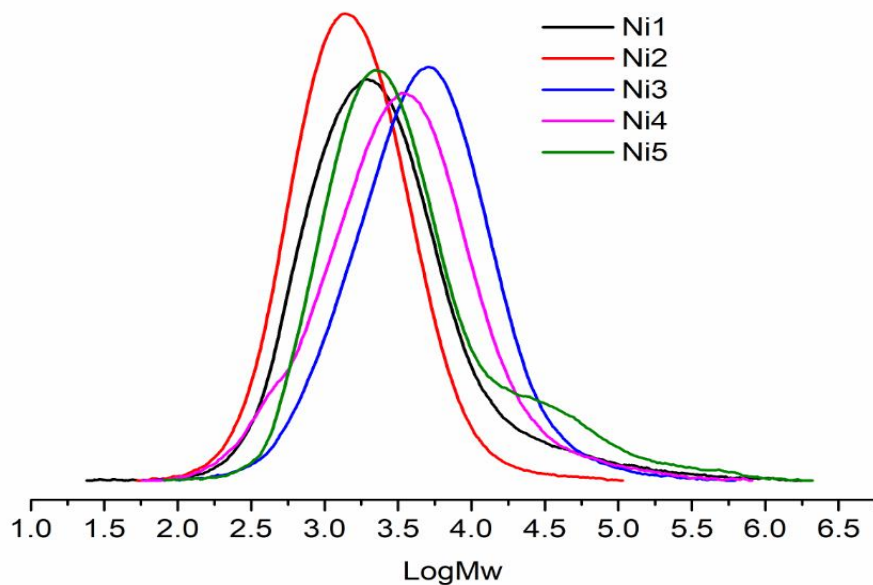


**Figure S5** GPC curves of the polyethylene produced using **Ni1 – Ni5**/MMAO under optimum conditions (runs 3, 16 – 19, Table 4).

Sample: M-T1R6  
Size: 5.3400 mg  
Method: wsl

DSC

File: D:\DSCQ2000\sunwenhua\DESUM-T1R6.001

Run Date: 15-Oct-2021 15:12  
Instrument: DSC Q2000 V24.11 Build 124

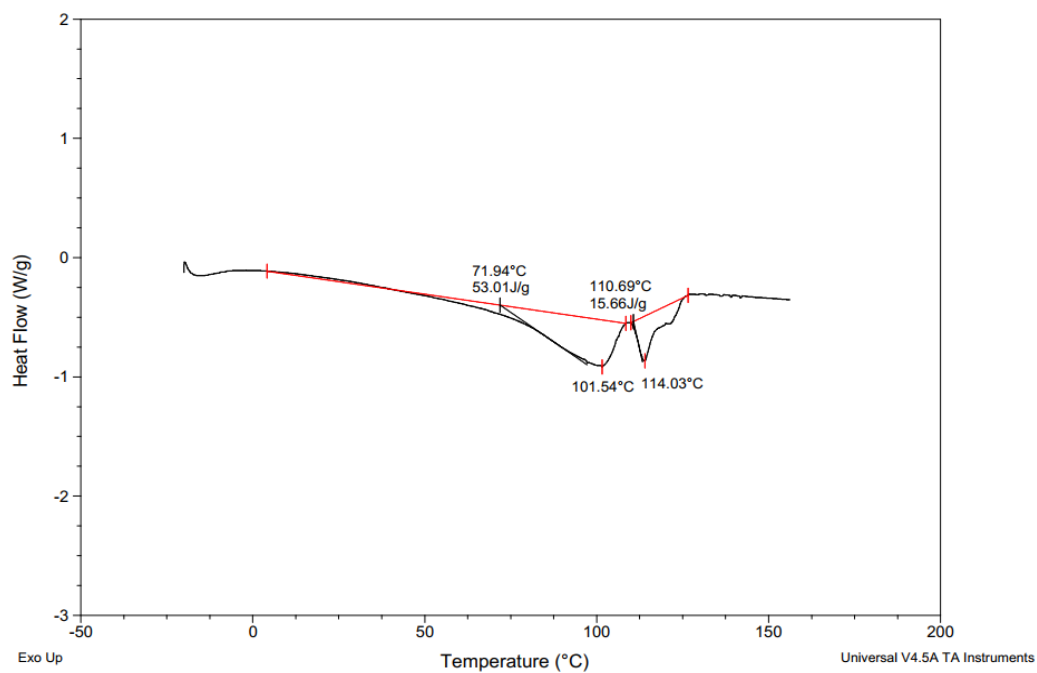


**Figure S6** DSC thermogram of the polyethylene produced using **Ni4**/MMAO (run 4, Table 4).

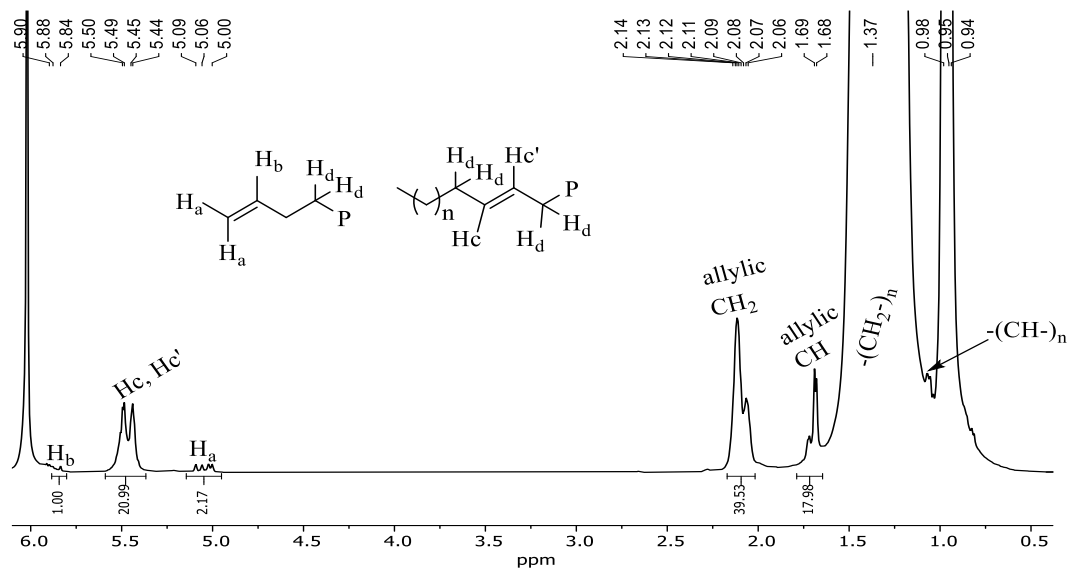


**Figure S7**  $^1H$  NMR spectrum of the polyethylene sample produced using **Ni4**/MMAO at 30 °C (run 3, Table 4); recorded at 100 °C in  $d-C_2D_2Cl_4$ .

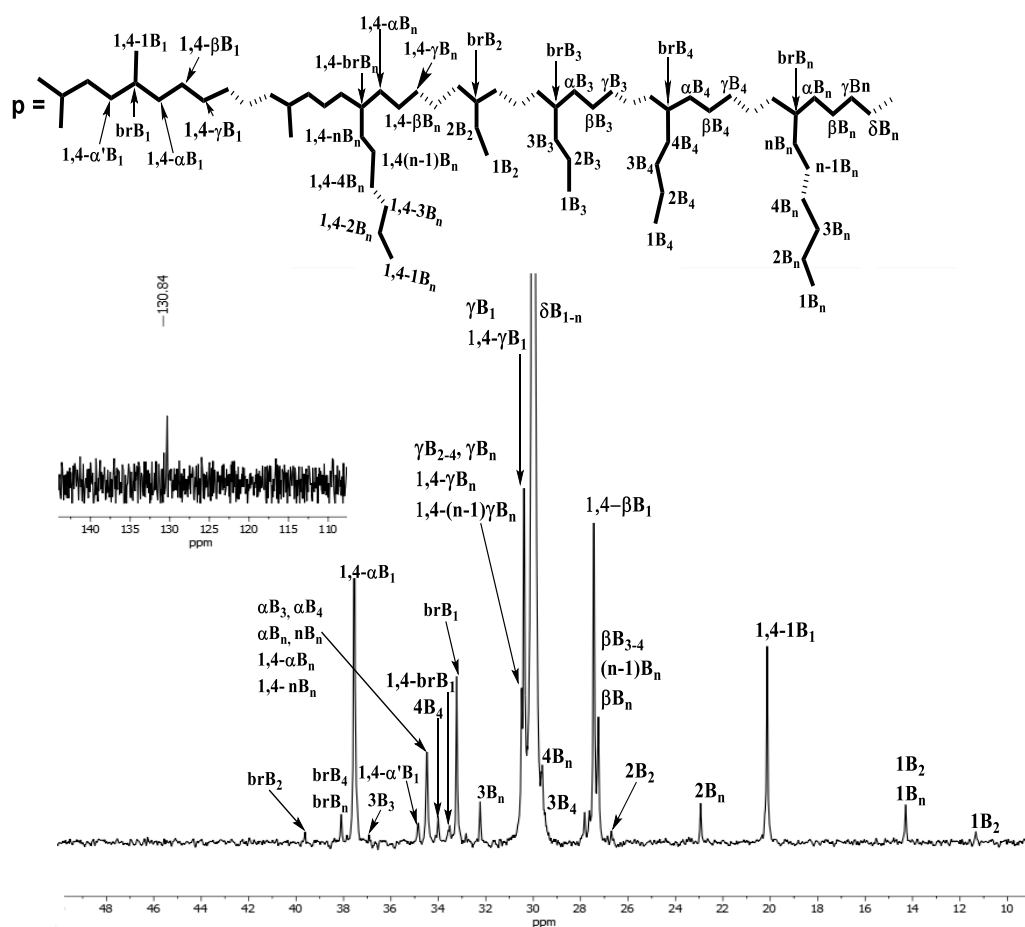


**Figure S8**  $^{13}\text{C}$  NMR spectrum of the polyethylene sample produced using Ni4/MMAO at 30 °C, including an inset of the  $\delta$  110–150 ppm region and a segment of the assigned polymer backbone (run 3, Table 4); recorded at 100 °C in  $d\text{-C}_2\text{D}_2\text{Cl}_4$ .



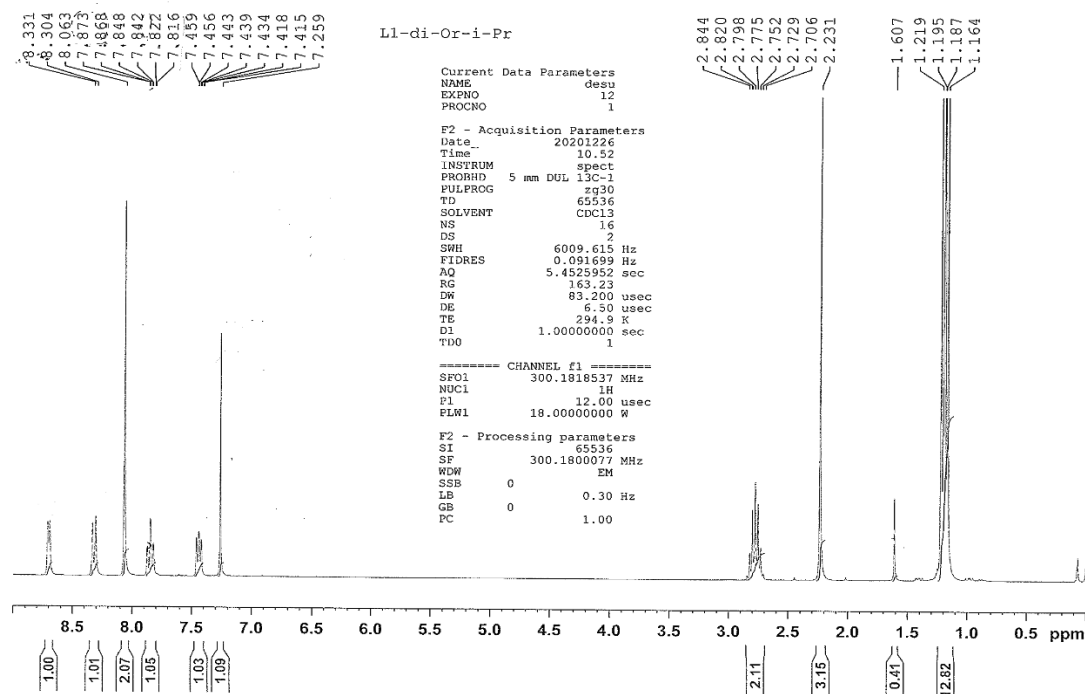


**Figure S9a**  $^1\text{H}$  NMR spectrum of ligand **L1**; recorded in  $\text{CDCl}_3$  at ambient temperature.

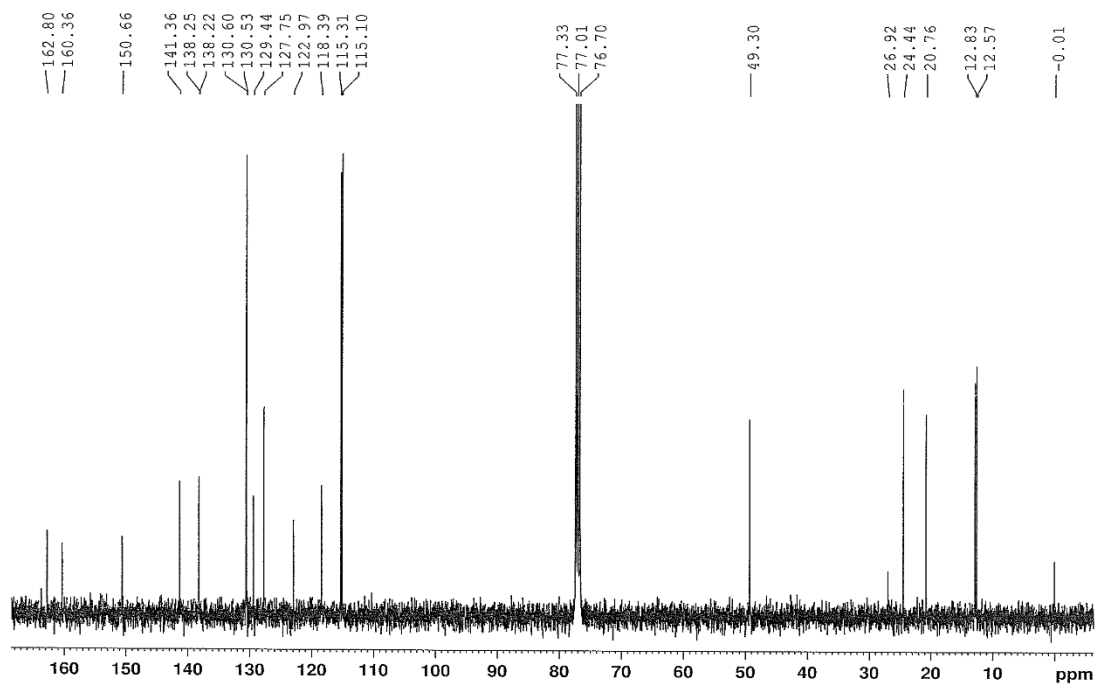


**Figure S9b**  $^{13}\text{C}$  NMR spectrum of ligand **L1**; recorded in  $\text{CDCl}_3$  at ambient temperature.

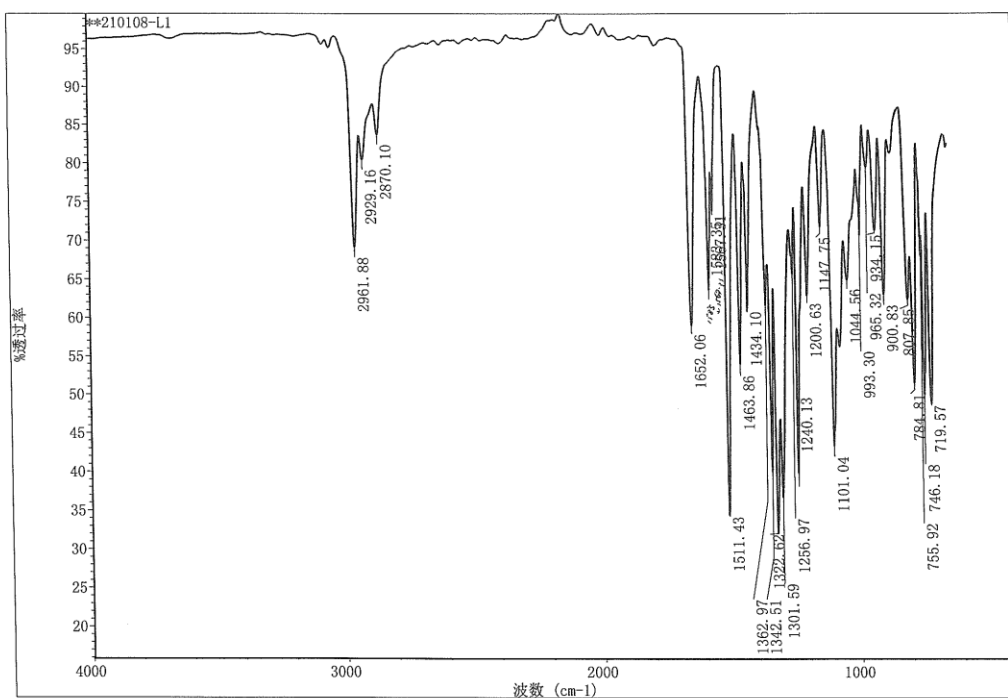


**Figure S10a** FTIR spectrum of ligand L1.

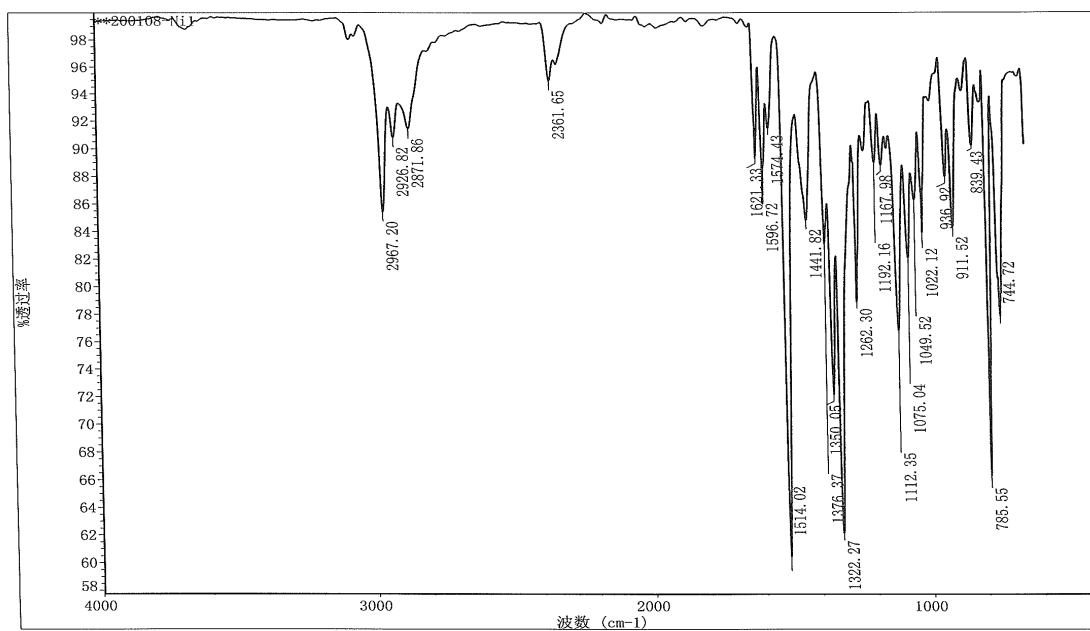


**Figure S10b** FTIR spectrum of complex Ni1.

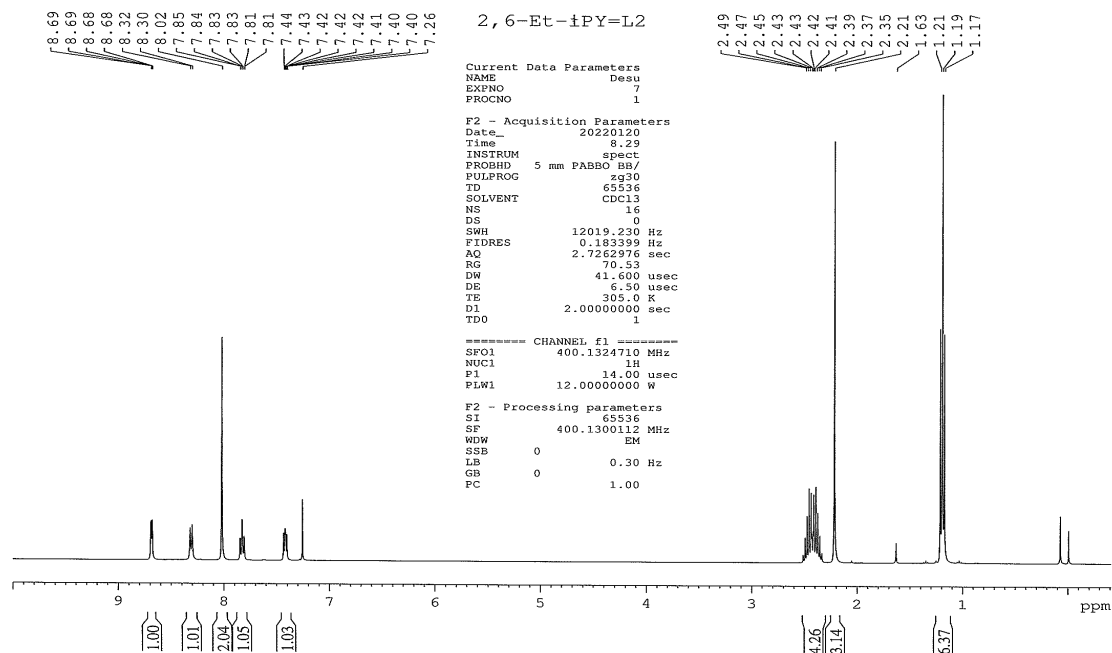


**Figure S11a**  $^1\text{H}$  NMR spectrum of ligand **L2**; recorded in  $\text{CDCl}_3$  at ambient temperature.

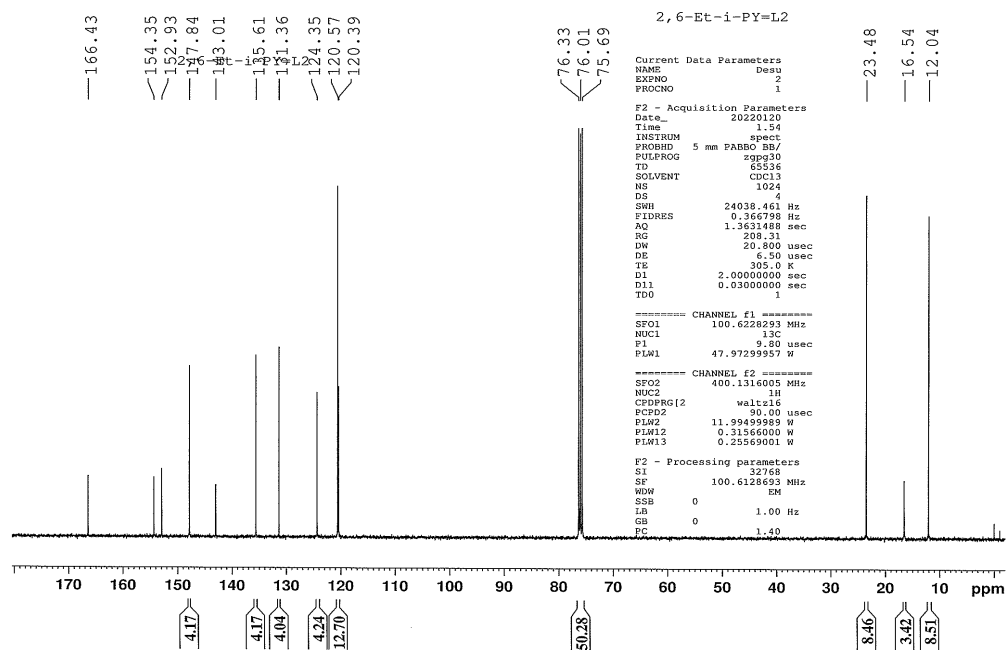


**Figure S11b**  $^{13}\text{C}$  NMR spectrum of ligand **L2**; recorded in  $\text{CDCl}_3$  at ambient temperature.

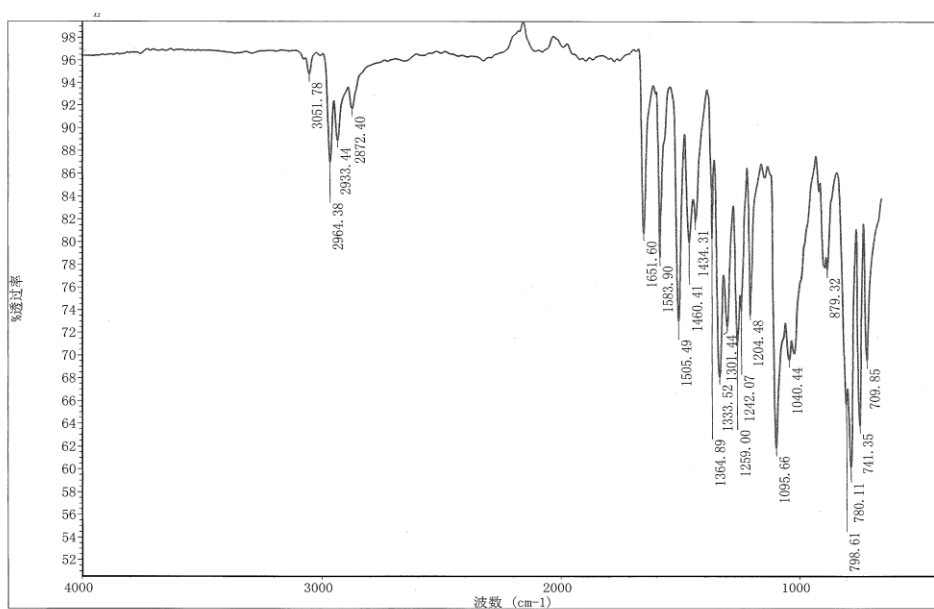


**Figure S12a** FTIR spectrum of ligand **L2**.

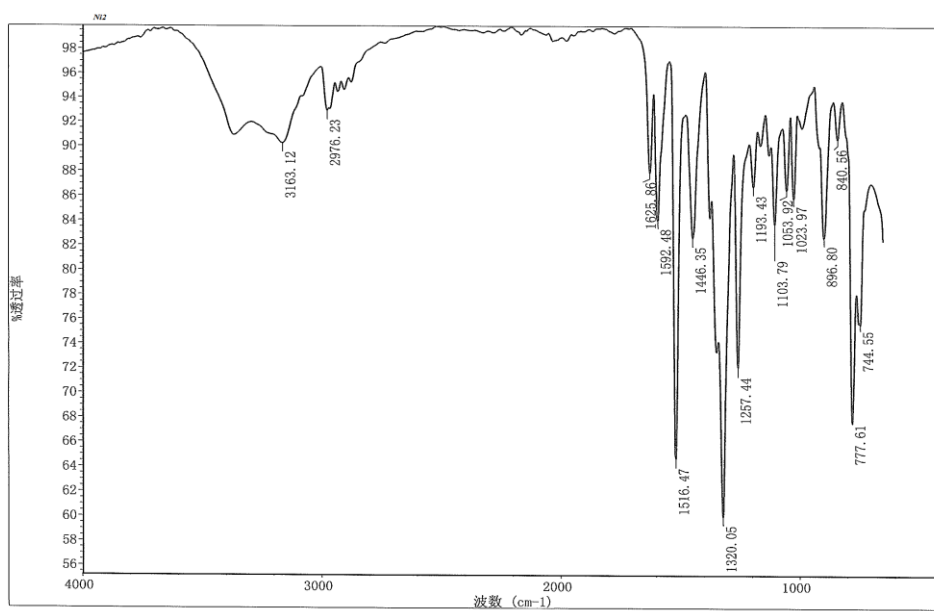


**Figure S12b** FTIR spectrum of complex **Ni2**.

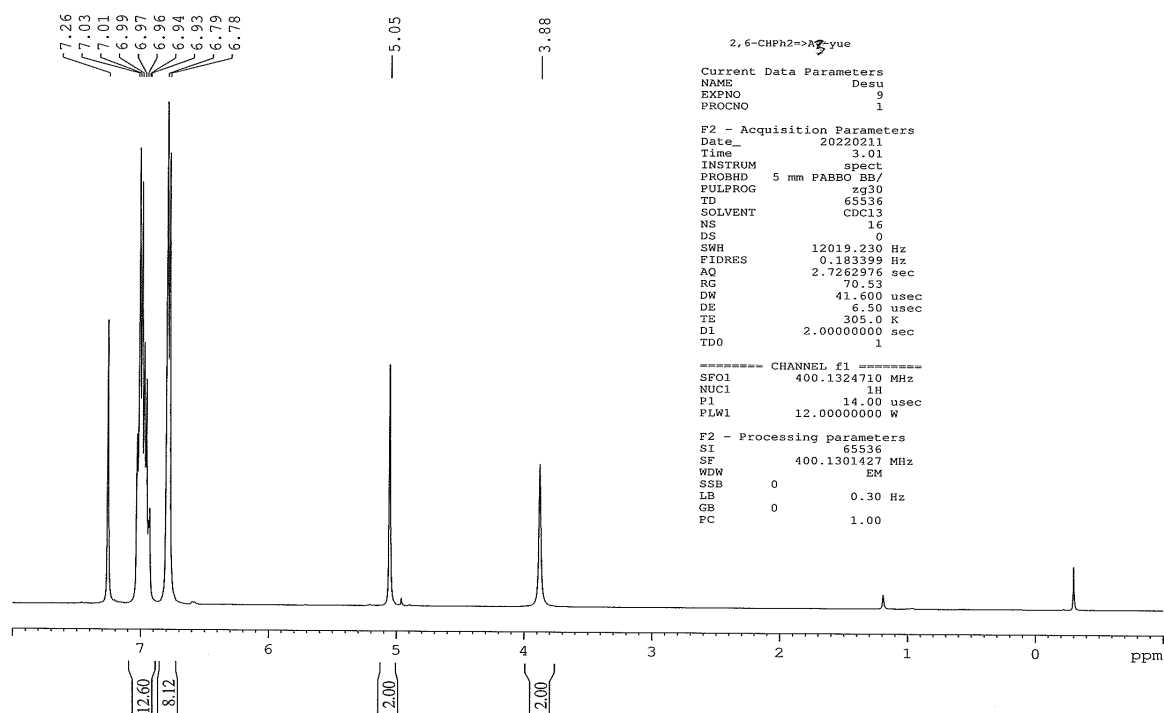


Figure S13  $^1\text{H}$  NMR spectrum of aniline **A3**; recorded in  $\text{CDCl}_3$  at ambient temperature.

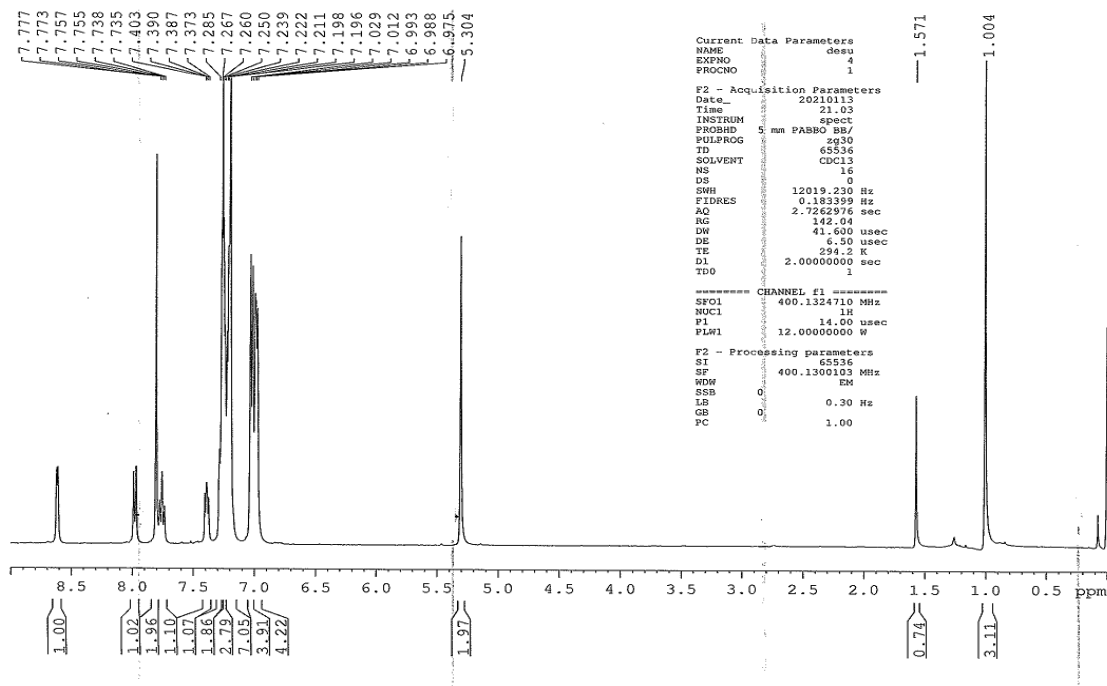
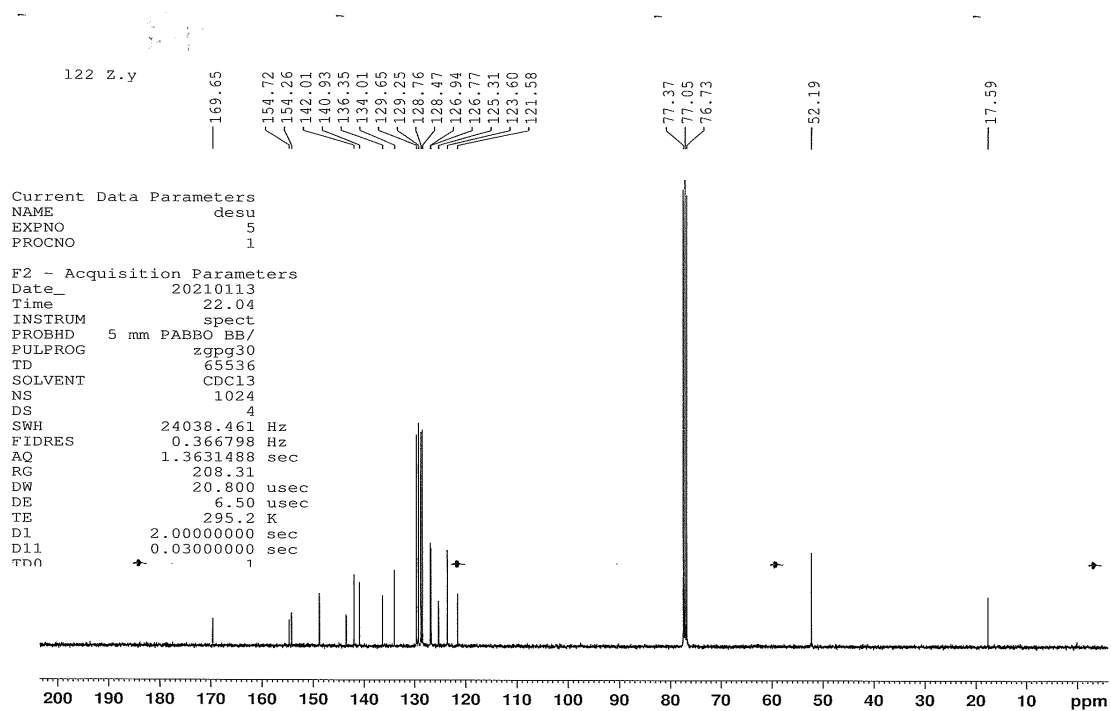
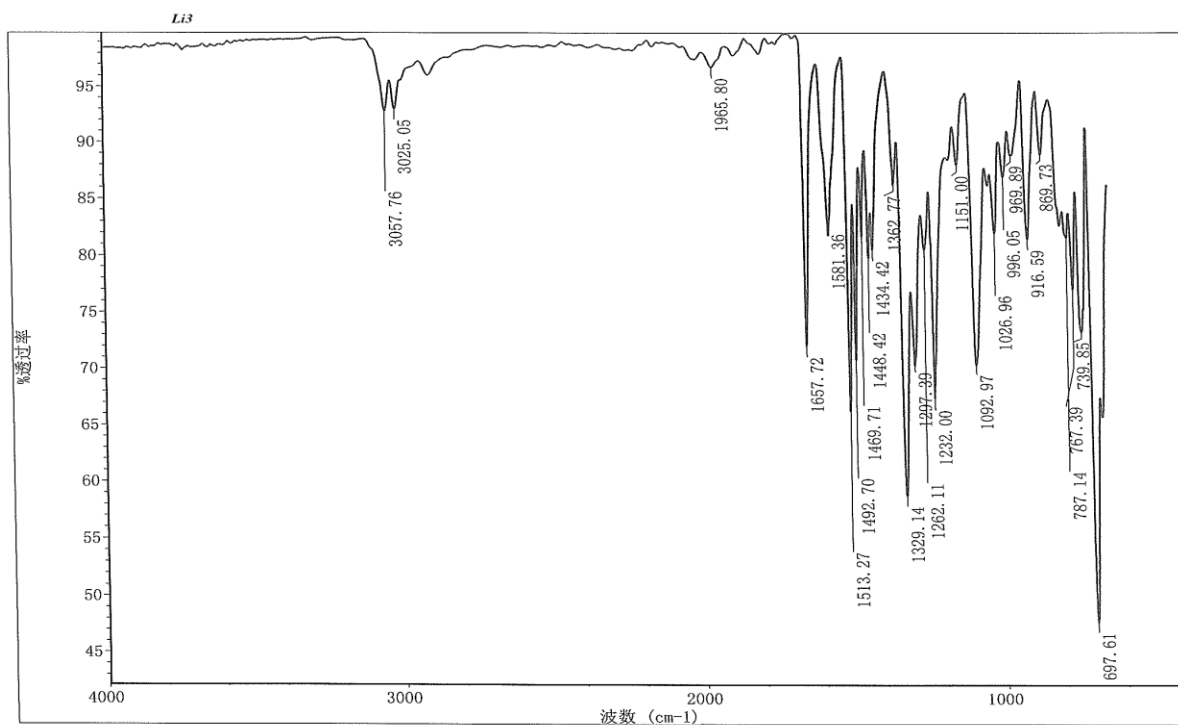


Figure S14a  $^1\text{H}$  NMR spectrum of ligand **L3**; recorded in  $\text{CDCl}_3$  at ambient temperature.



**Figure S14b**  $^{13}\text{C}$  NMR spectrum of ligand **L3**; recorded in  $\text{CDCl}_3$  at ambient temperature.



**Figure S15a** FTIR spectrum of ligand **L3**.

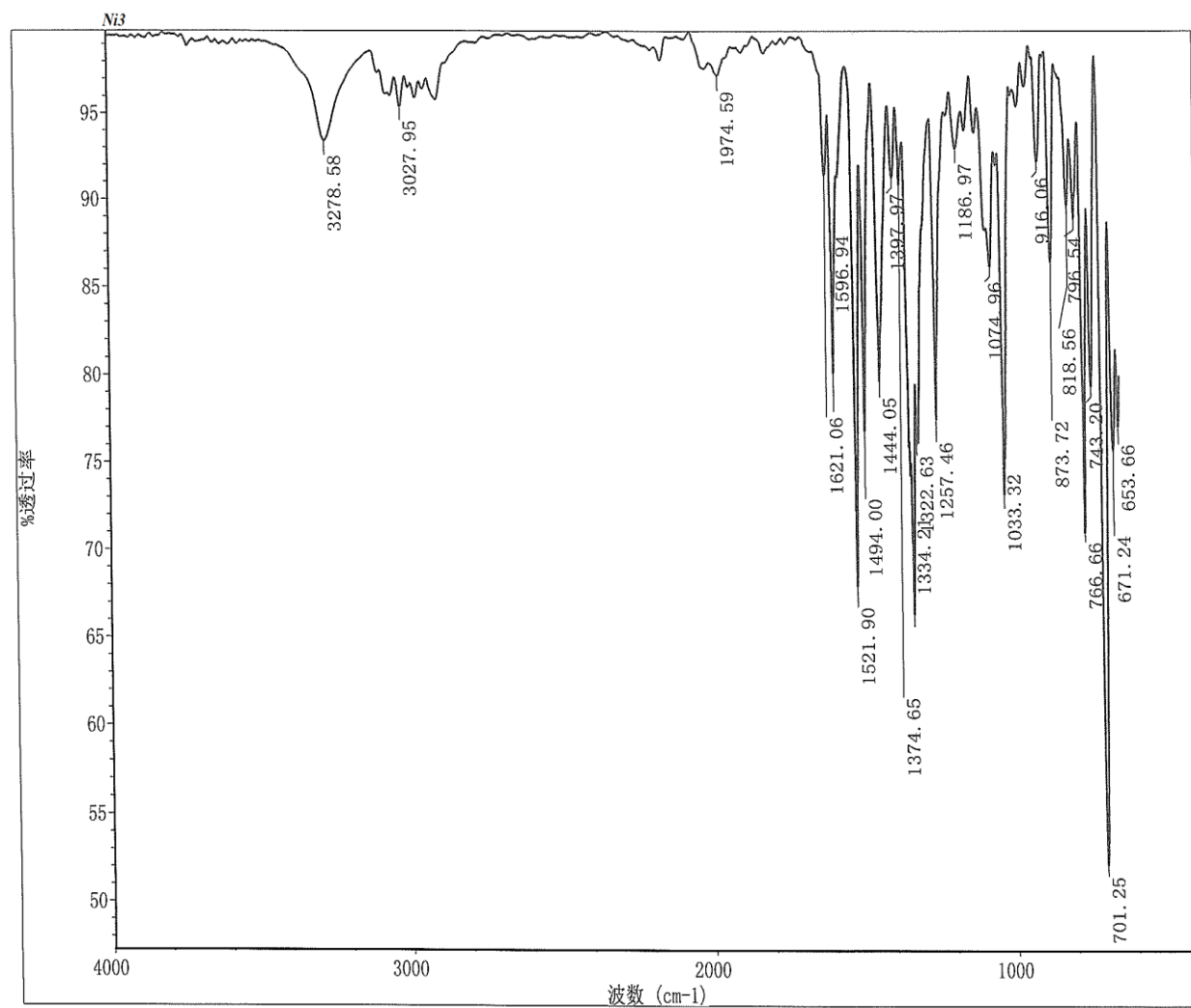


**Figure S15b** FTIR spectrum of complex **Ni3**.

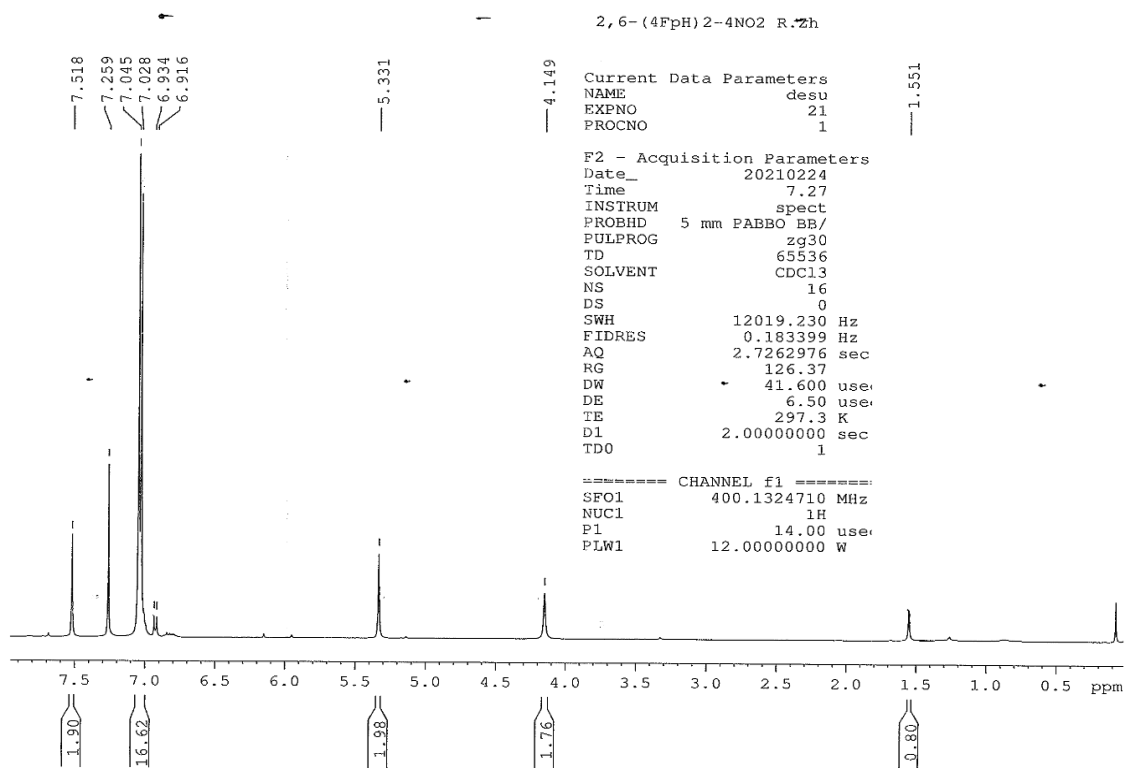


**Figure S16**  $^1\text{H}$  NMR spectrum of aniline **A4**; recorded in  $\text{CDCl}_3$  at ambient temperature.

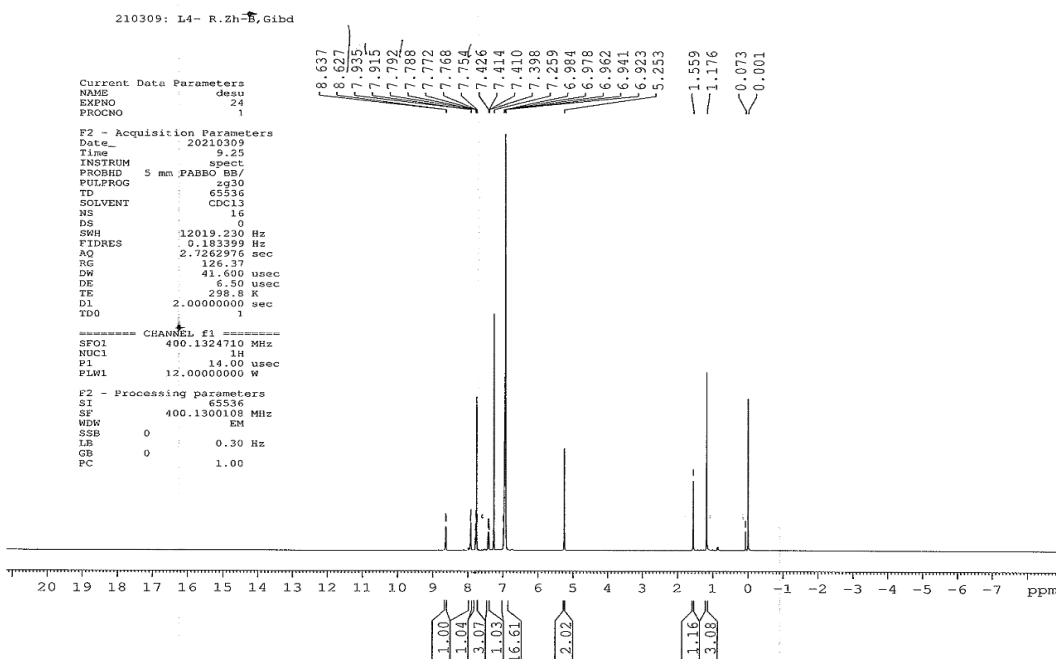


**Figure S17a**  $^1\text{H}$  NMR spectrum of ligand **L4**; recorded in  $\text{CDCl}_3$  at ambient temperature.



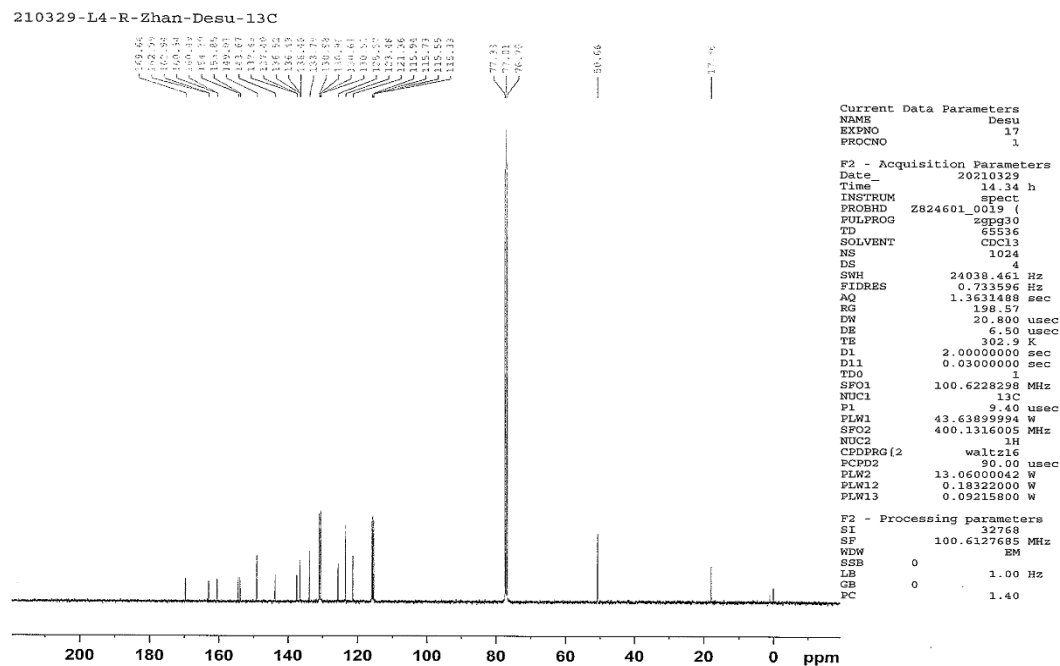


Figure S17b  $^{13}\text{C}$  NMR spectrum of ligand **L4**; recorded in  $\text{CDCl}_3$  at ambient temperature.

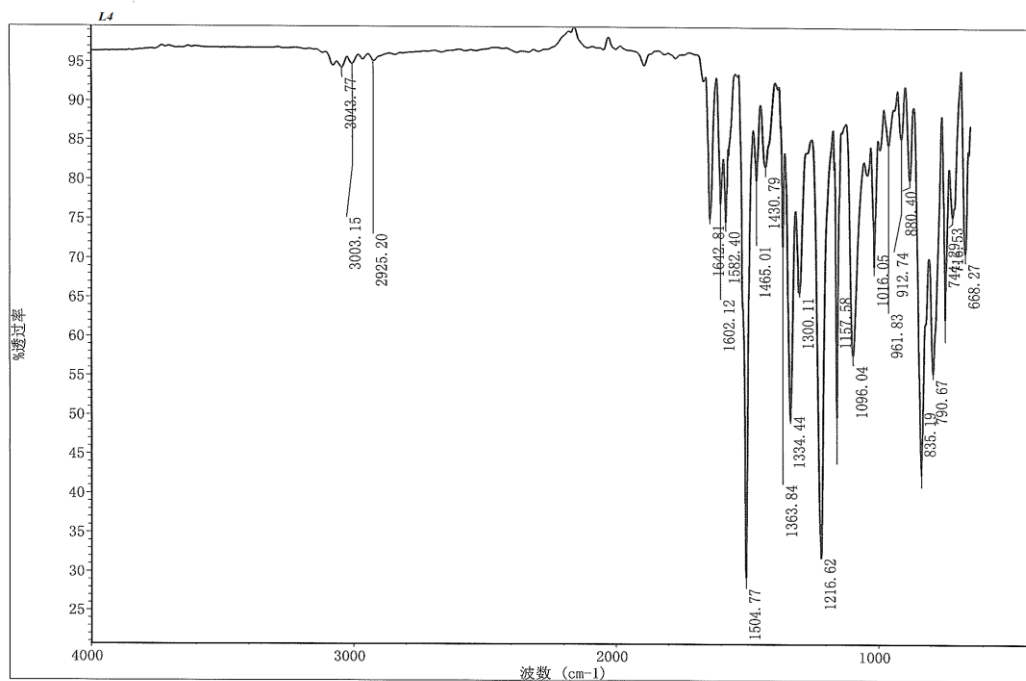
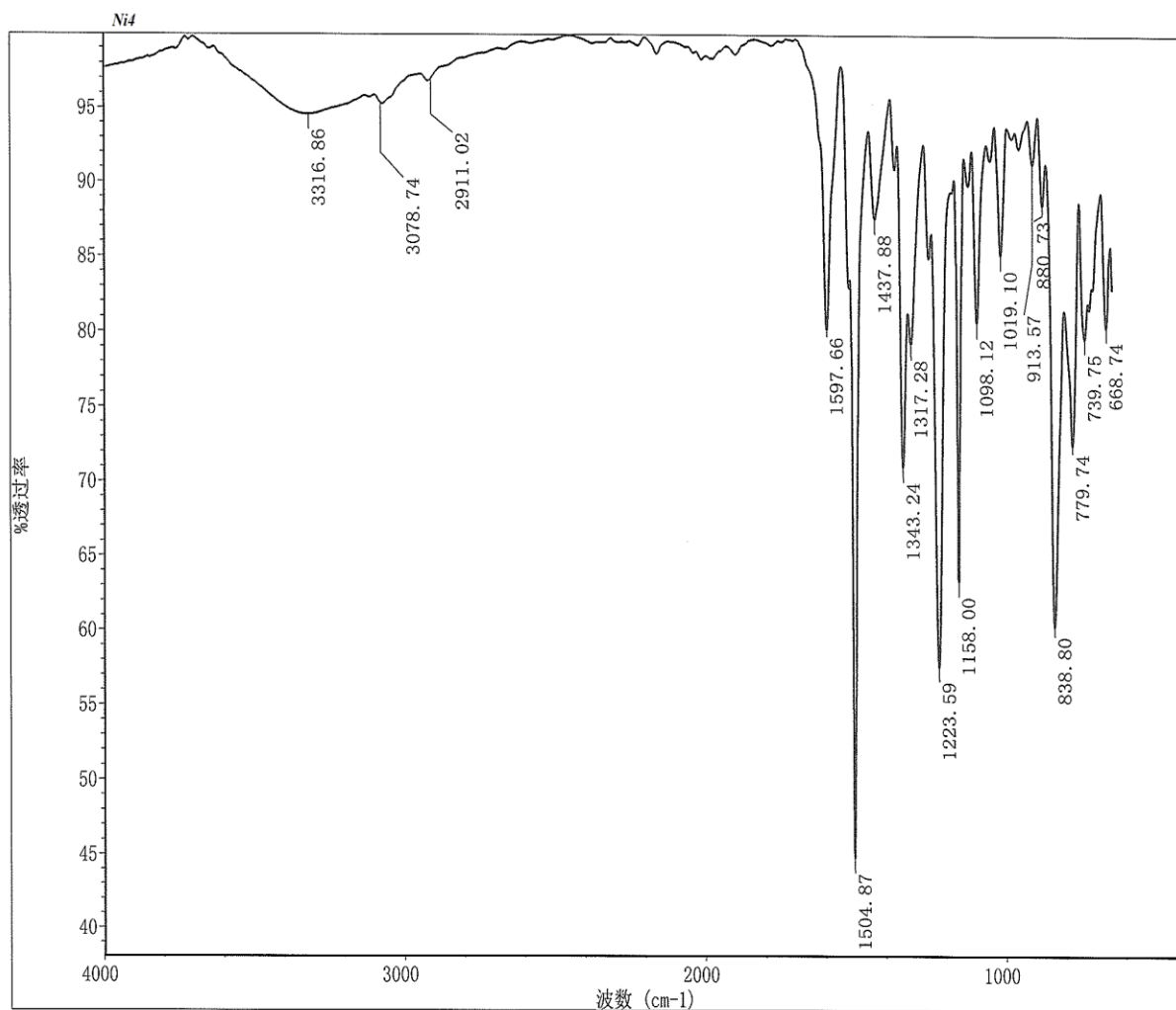
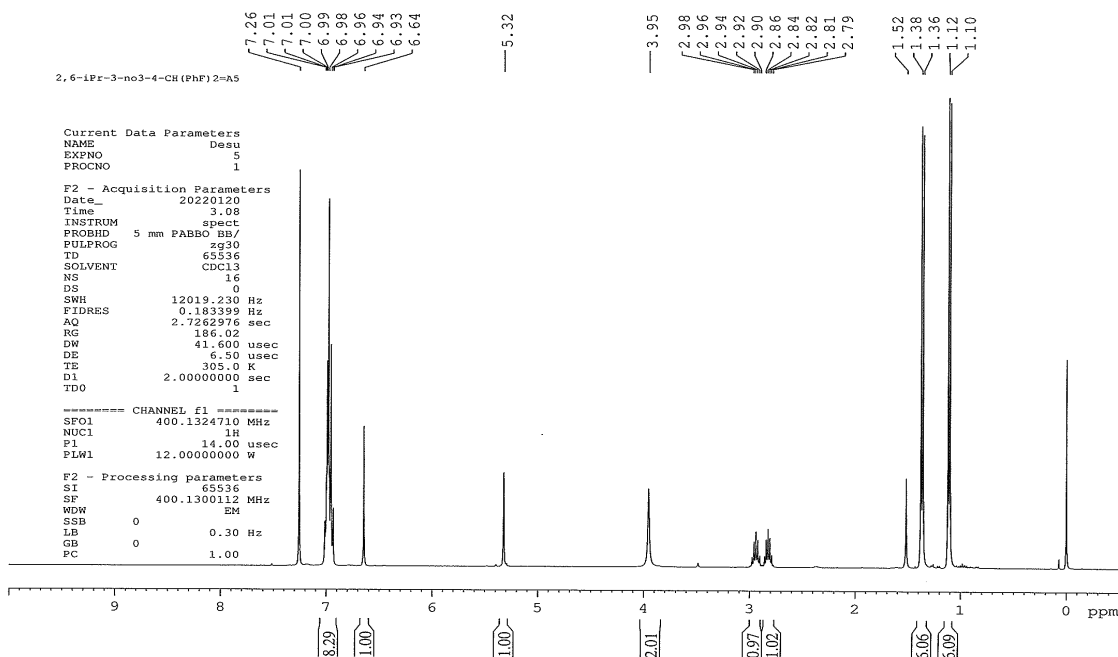


Figure S18a FTIR spectrum of ligand **L4**.



**Figure S18b** FTIR spectrum of complex **Ni4**.



**Figure S19a**  $^1\text{H}$  NMR spectrum of aniline **A5**; recorded in  $\text{CDCl}_3$  at ambient temperature.

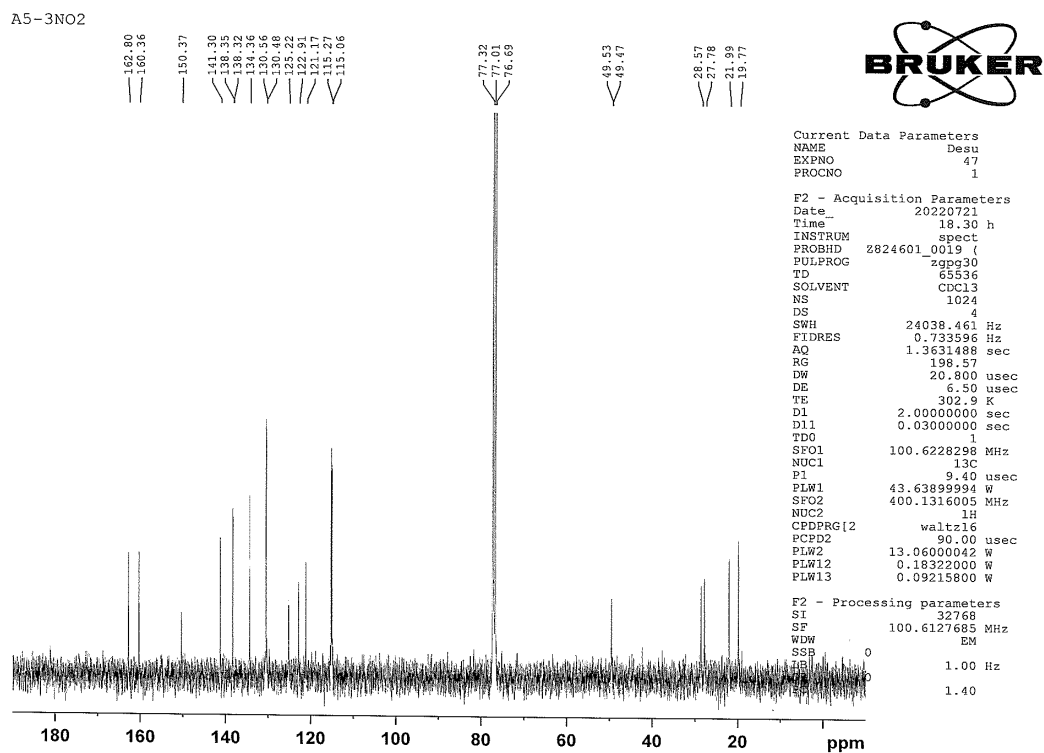


**Figure S19b**  $^{13}\text{C}$  NMR spectrum of aniline **A5**; recorded in  $\text{CDCl}_3$  at ambient temperature.

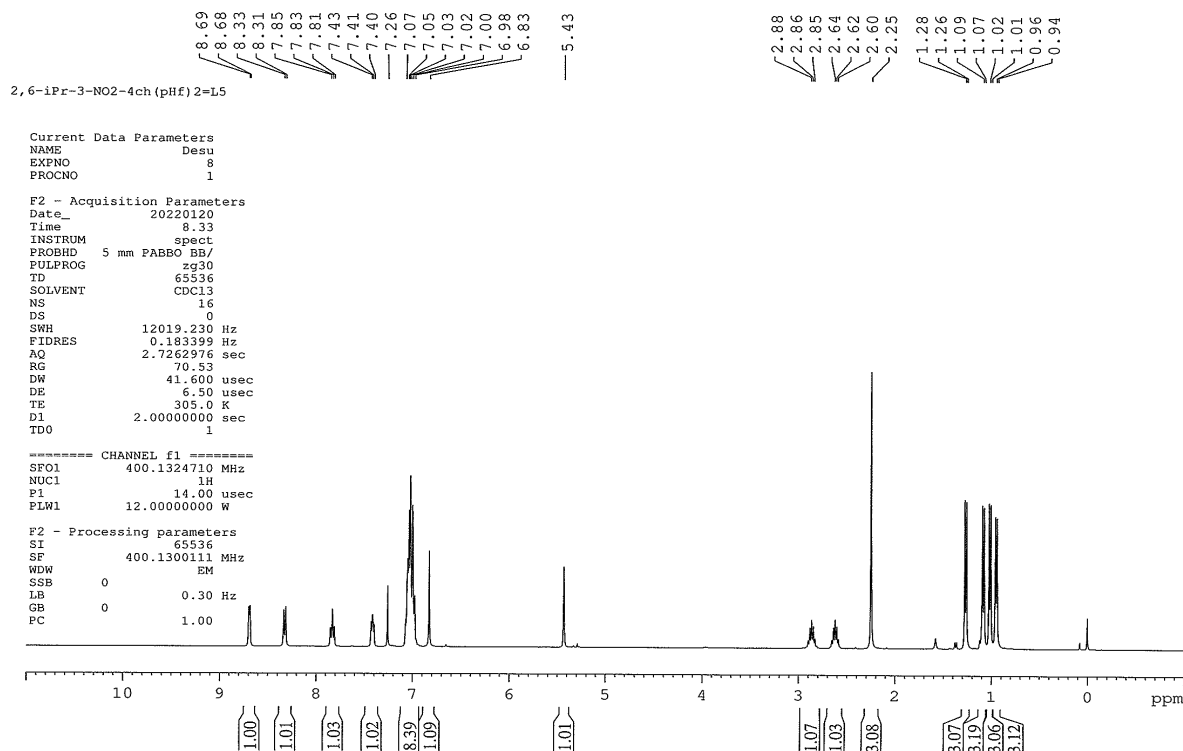


**Figure S20a**  $^1\text{H}$  NMR spectrum of ligand **L5**; recorded in  $\text{CDCl}_3$  at ambient temperature.

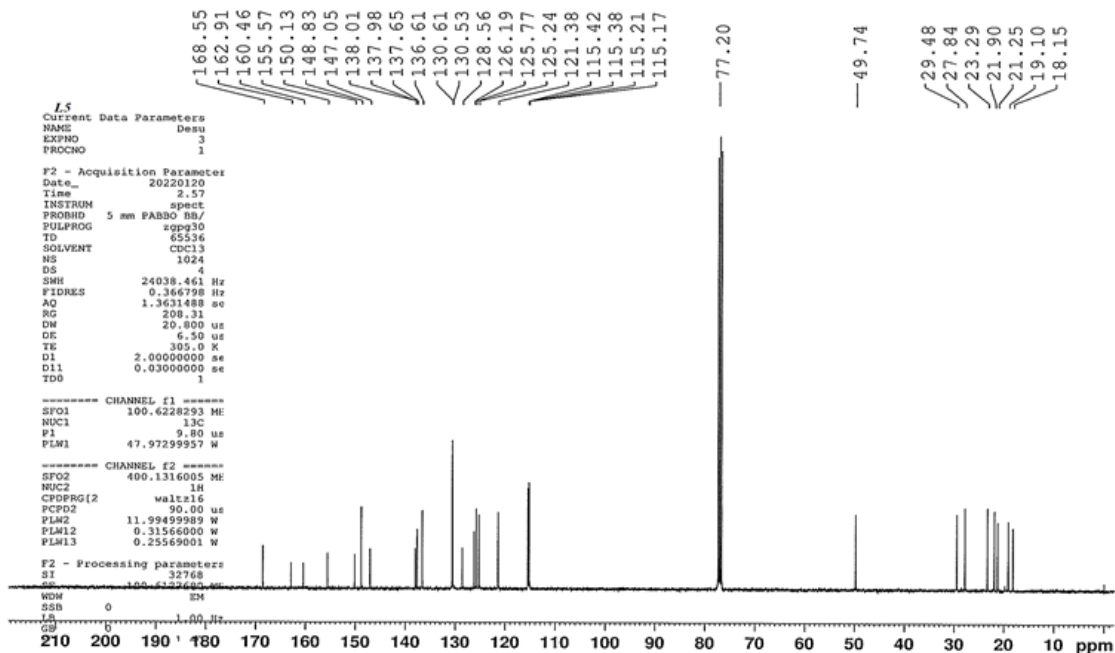


**Figure S20b**  $^{13}\text{C}$  NMR spectrum of ligand **L5**; recorded in  $\text{CDCl}_3$  at ambient temperature.

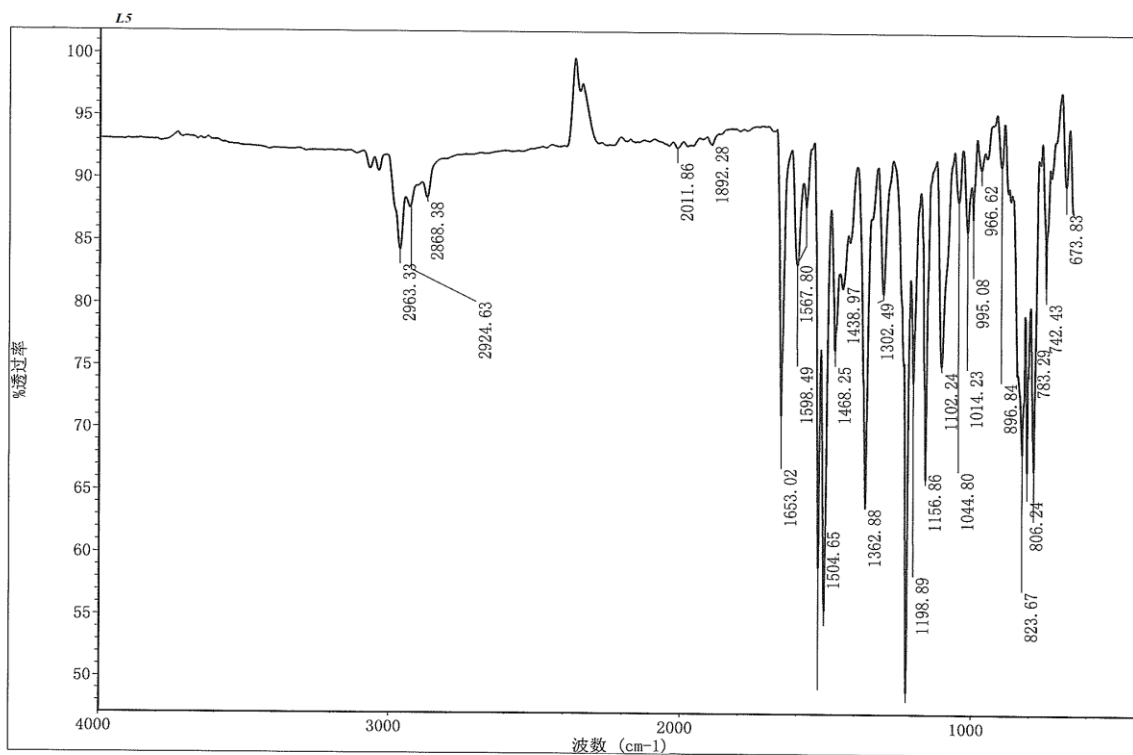


**Figure S21a** FTIR spectrum of ligand **L5**.

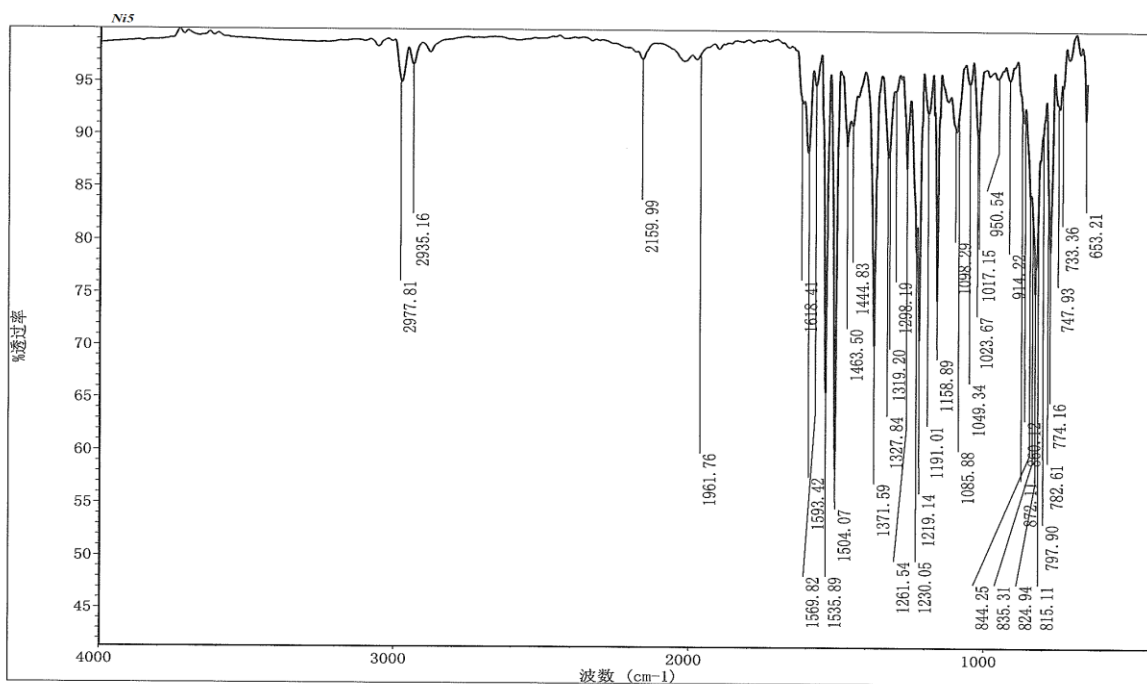


**Figure S21b** FTIR spectrum of complex **Ni5**.

**Table S1** Crystallographic data for **Ni3**·xH<sub>2</sub>O (x = 2,3), **Ni4** and **Ni5**.

	<b>Ni3</b> ·xH <sub>2</sub> O (x = 2,3)	<b>Ni4</b>	<b>Ni5</b>
Identification code			
CCDC No.	2195148	2195149	2195150
Empirical formula	C <sub>117</sub> H <sub>109</sub> Br <sub>6</sub> N <sub>9</sub> Ni <sub>3</sub> O <sub>14</sub> ·3CH <sub>2</sub> Cl <sub>2</sub>	C <sub>39</sub> H <sub>27</sub> N <sub>3</sub> Br <sub>2</sub> O <sub>2</sub> F <sub>4</sub> Ni	C <sub>32</sub> H <sub>31</sub> N <sub>3</sub> Br <sub>2</sub> O <sub>2</sub> F <sub>2</sub> Ni
Formula weight	2775.49	864.16	746.13
Temperature/K	170.00(12)	170.00(13)	170.00(11)
Crystal system	monoclinic	triclinic	triclinic
Space group	P2 <sub>1</sub> /n	P-1	P-1
a/Å	17.20860(10)	11.9377(4)	10.7461(2)
b/Å	21.93390(10)	12.5497(4)	11.2319(2)
c/Å	35.0020(2)	16.0360(4)	13.9891(2)
α/°	90	78.123(2)	102.7970(10)
β/°	94.9920(10)	71.397(3)	105.9090(10)
γ/°	90	75.959(3)	96.0270(10)
Volume/Å <sup>3</sup>	13161.45(12)	2187.23(12)	1558.55(5)
Z	4	2	2
ρ <sub>calc</sub> /cm <sup>3</sup>	1.401	1.312	1.590
μ/mm <sup>-1</sup>	4.230	3.201	4.283
F(000)	5624.0	864.0	752.0
Crystal size/mm <sup>3</sup>	0.15 × 0.06 × 0.05	0.15 × 0.1 × 0.06	0.4 × 0.3 × 0.2
Radiation	Cu Kα (λ = 1.54184)	Cu Kα (λ = 1.54184)	Cu Kα (λ = 1.54184)
2θ range for data collection/°	5.542 to 150.778	5.872 to 151.358	6.808 to 150.482
Index ranges	-21 ≤ h ≤ 21, -22 ≤ k ≤ 27, -43 ≤ l ≤ 42	-14 ≤ h ≤ 14, -14 ≤ k ≤ 15, -15 ≤ l ≤ 19	-13 ≤ h ≤ 13, -14 ≤ k ≤ 14, -16 ≤ l ≤ 17
Reflections collected	103711	27525	18282
Independent reflections	26087 [R <sub>int</sub> = 0.0355, R <sub>sigma</sub> = 0.0301]	8656 [R <sub>int</sub> = 0.0577, R <sub>sigma</sub> = 0.0445]	6159 [R <sub>int</sub> = 0.0209, R <sub>sigma</sub> = 0.0161]
Data/restraints/parameters	26087/132/1525	8656/0/461	6159/0/384
Goodness-of-fit on F <sup>2</sup>	1.019	1.073	1.091
Final R indexes [I ≥ 2σ (I)]	R <sub>1</sub> = 0.0397, wR <sub>2</sub> = 0.1028	R <sub>1</sub> = 0.0745, wR <sub>2</sub> = 0.2096	R <sub>1</sub> = 0.0325, wR <sub>2</sub> = 0.0850
Final R indexes [all data]	R <sub>1</sub> = 0.0445, wR <sub>2</sub> = 0.1059	R <sub>1</sub> = 0.0813, wR <sub>2</sub> = 0.2177	R <sub>1</sub> = 0.0331, wR <sub>2</sub> = 0.0855
Largest diff. peak/hole / e Å <sup>-3</sup>	1.53/-1.94	2.06/-1.74	0.76/-0.89

**Table S2**  $^{13}\text{C}$  NMR data of the polyethylene sample produced using **Ni4**/EtAlCl<sub>2</sub> at 30 °C (run 3, Table 3).

Peak no.	Chemical shift (ppm)	Experimental integration	Peak no.	Chemical shift (ppm)	Experimental integration
1	11.31	0.1	18	30.48	1.4
2	14.27	1	19	31.68	0
3	14.77	0.54	20	32.23	0.97
4	19.86	0.12	21	32.72	0.44
5	20.12	3.29	22	33.22	2.4
6	20.33	0	23	33.57	0.42
7	22.93	0.77	24	33.83	0
8	23.42	0	25	34.01	0.63
9	24.67	0	26	34.5	0.97
10	26.72	0.3	27	34.87	0.5
11	27.26	1.72	28	36.94	0
12	27.44	5.74	29	37.55	6.8
13	27.83	0.73	30	37.86	0
14	29.53	1.24	31	38.11	0.42
15	29.61	2.62	32	38.37	0
16	30	126.51	33	39.62	0
17	30.38	6.68			

**Table S3** Branching analysis for the polyethylene sample produced using **Ni4**/EtAlCl<sub>2</sub> at 30 °C (run 3, Table 3) [S5].

Branching content		Relative percentage (%)
N <sub>M</sub>	7.715	67.97
N <sub>E</sub>	0.33	2.90
N <sub>P</sub>	0.64	5.64
N <sub>B</sub>	0.5	4.40
N <sub>A</sub>	0	0
N <sub>M(1,4)</sub>	0.75	6.61
N <sub>M(1,5)</sub>	0	0
N <sub>M(1,6)</sub>	0.435	3.83
N <sub>L</sub>	0.98	8.63
N <sub>L(1,4)</sub>	0	0
[E]	105.475	
[R]	11.35	100 %
Total branches		<b>48/1000 Cs %</b>
Methyl branches		78.41
Ethyl branches		2.91
Propyl branches		5.64
Butyl branches		4.41
Amyl branches		0
Longer branches		8.63



**Table S4** <sup>13</sup>C NMR data of the polyethylene sample with Ni4/MMAO at 30 °C (run 3, Table 4).

Peak no.	Chemical shift (ppm)	Experimental integration	Peak no.	Chemical shift (ppm)	Experimental integration
1	11.34	0.23	18	30.49	4.06
2	14.29	1	19	31.68	0
3	14.77	0	20	32.24	0.9
4	19.86	0	21	32.72	0
5	20.13	5.46	22	33.22	4.29
6	20.33	0	23	33.52	0.68
7	22.94	0.94	24	33.83	0
8	23.42	0	25	34.01	0.79
9	24.67	0	26	34.49	3.32
10	26.7	0.21	27	34.85	0.63
11	27.25	3.98	28	36.94	0.85
12	27.44	10.81	29	37.54	11.22
13	27.83	0.94	30	37.86	0
14	29.53	1.3	31	38.1	0.68
15	29.62	2.77	32	38.37	0
16	30	174.11	33	39.62	0.18
17	30.38	10.66		-	-

**Table S5** Branching analysis for the polyethylene sample produced using **Ni4**/MMAO at 30 °C (run 3, Table 4) [S5].

Branching content		Relative percentage (%)
N <sub>M</sub>	10.0125	75.61
N <sub>E</sub>	0.13	0.98
N <sub>P</sub>	0.85	6.42
N <sub>B</sub>	0.395	2.98
NA	0	0
N <sub>M(1,4)</sub>	0.485	3.66
N <sub>M(1,5)</sub>	0	0
N <sub>M(1,6)</sub>	0.47	3.55
N <sub>L</sub>	0.9	6.80
N <sub>L(1,4)</sub>	0	0
[E]	86.6	
[R]	13.2425	100%
Total branches		<b>66/1000 Cs</b>
Methyl branches		82.82
Ethyl branches		0.98
Propyl branches		6.42
Butyl branches		2.98
Amyl branches		0
Longer branches		6.80

## References

- S1. Muller, T. E.; Hultsch, K. C.; Yus, M.; Foubelo, F.; Tada, M. Hydroamination: Direct Addition of Amines to Alkenes and Alkynes. *Chem. Rev.* **2008**, 108, 3795-3892.
- S2. Meiries, S.; Speck, K.; Cordes, D. B.; Slawin, A. M.; Nolan, S. P. [Pd(IPr\*<sup>OMe</sup>)(acac)Cl]: Tuning the N-Heterocyclic Carbene in Catalytic C–N Bond Formation. *Organometallics* **2013**, 32, 330-339.
- S3. Zhang, R.; Wang, Z.; Ma, Y.; Solan, G. A.; Sun, Y.; Sun, W.-H. *Dalton Trans.* **2019**, 48, 1878-1891.
- S4. Mahmood, Q.; Zeng, Y.; Wang, X.; Sun, Y.; W.-H. Sun. Advancing polyethylene properties by incorporating –NO<sub>2</sub> moiety in 1,2-bis(arylimino)acenaphthyllylnickel precatalysts: Synthesis, characterization and ethylene polymerization. *Dalton Trans.* **2017**, 46, 6934 – 6947.
- S5. Galland, G. B.; de Souza, R. F.; Mauler R. S.; Nunes F. F. <sup>13</sup>C NMR determination of the composition of linear low-density polyethylene obtained with [η<sup>3</sup>-methallyl-nickel-diimine] PF<sub>6</sub> complex. *Macromolecules* **1999**, 32, 1620-1625.